REPORT DOCUMENTATION PAGE

Public reporting burden for the collection of information is estimated to average 1 hour per response, indicating the time for reviewing instructions, searching existing data sources, gathering and maintaining the data needed, and collecting and reviewing the collection of information. Send comments regarding this burden estimate or any other aspect of the collection of information, indicating suggestions for reducing this burden, to Washington Headquarters Services, Directorate for Information, Operations and Reports, 1215 Jefferson Davis Highway, Suite 1204, Arlington, VA 22202-4302, and to the Office of Management and Budget, Paperwork Reduction Project (0704-0183), Washington, D.C. 20503.

1. AGENCY USE ONLY (Leave blank)	2. REPORT DATE January 22, 1996	3. REPORT TYPE AND DATES COVERED Final Report: 1 December 1992 through 30 November 1995

4. TITLE AND SUBTITLE

Interaction of Complex Vorticity Fields with Aerodynamic Surfaces:
Sources of Buffeting-Induced Loading and Vibration

5. FUNDING NUMBERS

AFOSR F49620-93-1-0075,
P00001

6. AUTHOR(S)

Professor Donald Rockwell

7. PERFORMING ORGANIZATION NAME(S) AND ADDRESS(ES)

Department of Mechanical Engineering and Mechanics
Lehigh University
354 Packard Laboratory, 19 Memorial Drive West
Bethlehem, Pennsylvania 18015

AFOSR-TR-96

G151

9. SPONSORING/MONITORING AGENCY NAME(S) AND ADDRESS(ES)

Dr. L. Sakell
Aerospace and Materials Sciences Directorate
Air Force Office of Scientific Research (AFMC)
110 Duncan Avenue, Suite B115
Bolling Air Force Base, D. C. 20332-6448

N/A

DR. Len Sakell   2307 CS

10. SPONSORING/MONITORING AGENCY REPORT NUMBER

11. SUPPLEMENTARY NOTES

12a. DISTRIBUTION/AVAILABILITY STATEMENT

Approved for public release,
distribution unlimited

12b. DISTRIBUTION CODE

13. ABSTRACT (Maximum 200 words)

The central goal of this program is to determine the origin of unsteady loading on a fin or blade in terms of the instantaneous velocity and vorticity fields associated with an incident vortex. New techniques of high-image-density particle image velocimetry provide the first instantaneous, global representations of the crucial features of this class of flows. The basic mechanisms of distortion of quasi-two-dimensional and three-dimensional vortices, including the case of a broken-down vortex, as the vortex encounters the leading-edge of the fin or blade, provide fundamental insight into this class of flow-structure interaction. The instantaneous flow structure provides a basis for interpretation of time-averaged surface pressure and acceleration measurements obtained in both the present and previous investigations. Knowledge of the flow patterns is expected to lead, in turn, to new techniques for control of the unsteady loading.

19960404 042

14. SUBJECT TERMS

15. NUMBER OF PAGES 17
16. Price code

17. SECURITY CLASSIFICATION OF REPORT Unclassified	18. SECURITY CLASSIFICATION OF THIS PAGE Unclassified	19. SECURITY CLASSIFICATION OF ABSTRACT Unclassified	20. LIMITATION OF ABSTRACT

FINAL TECHNICAL REPORT FOR AFOSR GRANT

INTERACTION OF COMPLEX VORTICITY FIELDS WITH AERODYNAMIC SURFACES: SOURCES OF BUFFETING-INDUCED LOADING AND VIBRATION

P.I. Name: Rockwell, Donald O.
Institution: Lehigh University, 354 Packard Laboratory, 19 Memorial Drive West,
    Bethlehem, PA 18015
Contract/Grant No: F49620-93-1-0075, P00001
Effective Dates: 1 December 1992 through 30 November 1995

1. ABSTRACT

The central goal of this program is to determine the origin of unsteady loading on a fin or blade in terms of the instantaneous velocity and vorticity fields associated with an incident vortex. New techniques of high-image-density particle image velocimetry provide the first instantaneous, global representations of the crucial features of this class of flows. The basic mechanisms of distortion of quasi-two-dimensional and three-dimensional vortices, including the case of a broken-down vortex, as the vortex encounters the leading-edge of the fin or blade, provide fundamental insight into this class of flow-structure interaction. The instantaneous flow structure provides a basis for interpretation of time-averaged surface pressure and acceleration measurements obtained in both the present and previous investigations. Knowledge of the flow patterns is expected to lead, in turn, to new techniques for control of the unsteady loading.

2. EXPERIMENTAL SYSTEMS

Several new experimental systems have been developed. They include two-dimensional and three-dimensional (delta) wings with controllable pitch angle; plates and fins with multiple pressure sensors, allowing measurement of surface pressure; and laser conditioning, steering and scanning systems for high-image-density PIV measurements. All components, including image shifting and photographic systems, are controlled by a central microcomputer. New types of post-processing techniques allow, for the first time, spatial correlation of instantaneous vorticity concentrations. This and related approaches have provided the first insight into the relationship between the instantaneous flow structure and the time-averaged spectra of surface pressure fluctuations, acquired both in the present investigation and in previous wind tunnel tests.

Generation of the vortex incident upon the blade or fin is accomplished by prescribed motion of a two-dimensional or three-dimensional wing, forced by a high resolution computer-controlled motor, which receives commands from the central laboratory microcomputer. This approach allows arbitrary specification of the frequency and amplitude of the wing motion; in addition, arbitrary transient (ramp) motion is also attainable. In certain experiments, the upstream wing was not subjected to a prescribed

1

perturbation. The self-excited instability exhibited sufficient coherence in absence of applied perturbations.

The detailed interaction of the generated vortex with the blade or fin was determined by the PIV technique. Small, highly reflective spherical particles, having a nominal diameter of 12 microns were employed as seeding particles. They were illuminated with a scanning laser beam, originating from a continuous wave Argon-ion laser. The scan of the beam was accomplished by reflecting it from a multi-faceted polygonal mirror. Images were acquired using 35 mm film-based cameras, triggered by the central microcomputer. An essential element of this image acquisition system is a rotating mirror located directly in front of the camera lens. It imparted a constant displacement to all particles, allowing measurements in regions of reverse flow, and generally decreasing the dynamic range of the image displacements.

An extensive series of post-processing capabilities were developed during the course of this program. In addition to the classical representations of the instantaneous flow structure based on velocity, vorticity, and streamline patterns, spatial filtering techniques and methods for determining spatial correlations of the instantaneous vorticity were formulated and implemented. These approaches provide insight well beyond that attainable for pointwise velocity measurements, and form a basis for physical interpretation of time-averaged representations of surface pressure and acceleration.

3. ACCOMPLISHMENTS/NEW FINDINGS

This program has involved several successive investigations, which are briefly summarized in the following. In each case, the corresponding journal article is designated. Each article provides full details on the experimental system and techniques, and the principal findings. In cases where the lead author is a graduate student, the journal article represents a synopsis of the major advances, which are described in detail in the full thesis available from the Department of Mechanical Engineering and Mechanics at Lehigh University.

3.1 *INTERACTION OF THE STREAMWISE VORTEX WITH A THIN PLATE: A SOURCE OF TURBULENT BUFFETING (A. Mayori and D. Rockwell, 1994, AIAA Journal, Vol. 32, No. 10, pp. 2022-2029)*

The three-dimensional interaction of a streamwise vortex with a thin plate (Figure 1) is investigated experimentally using high-image-density particle image velocimetry, which allows determination of the instantaneous streamline patterns and distributions of vorticity over entire planes of the flow. These representations of the flow reveal that the vortex-plate encounter generates a new type of vortex splitting, leading to two smaller-scale concentrations of streamwise vorticity (Figure 2). Their trajectories rapidly diverge from the plane of symmetry of the plate (Figure 3). Details of this encounter process are interpreted using instantaneous values of circulation, two-dimensional vorticity correlation functions and length scales of the vorticity field.

More specifically, the principal findings of this investigation are:

(1) The flow patterns in the crossflow plane, in particular the contours of constant streamwise vorticity, show that the incident, broken-down vortex exhibits substantial undulations and distortions with time. Nevertheless, underlying patterns of flow structure are evident. Most importantly, the incident vortex is split into two smaller-scale ones, which move away from the surface and the plane of symmetry of the plate. They encounter each other downstream of the trailing-edge; however, due to the interaction of the split vortices, their identity is rapidly lost in favor of highly chaotic motion.

(2) Regarding the concentrations of azimuthal vorticity, they are rapidly distorted as they encounter the leading-edge of the plate and move downstream along its surface. Immediately downstream of the trailing-edge, an embedded Kármán vortex street is detectable. Moreover, an array of vortices oriented orthogonally to the axis of the plate is also generated; this array arises from the recombination of the split vortices near the trailing-edge.

(3) The foregoing alterations of the instantaneous and time-averaged streamwise and azimuthal vorticity distributions are characterized in terms of circulation, three-dimensional surfaces of vorticity correlation functions, and length-scales of the vorticity concentrations. The circulation and length scales of the incident vortex decrease drastically due to the vortex-plate interaction.

(4) Moreover, it is demonstrated that control of the vorticity concentrations within the incident, broken-down vortex is attainable. Substantially smaller-scale vortices, relative to those occurring naturally, suggest a decreased correlation of the surface loading of the plate. Further exploration of control measures is called for, accounting for possible effects of Reynolds number on the detailed structure of the vorticity distributions.

(5) From a practical standpoint, the details of the vortex-plate interaction process revealed here can provide a physical basis for, and serve as a preliminary guide to, the magnitude and correlation of the unsteady surface pressure field. Furthermore, the fact that the encounter process, which occurs over a plate having a chord corresponding to only four diameters of the incident vortex, suggests that aerodynamic surfaces having small chord can be employed to mitigate larger-scale, coherent vortex activity.

3.2 BUFFETING AT THE LEADING-EDGE OF A FLAT PLATE DUE TO A STREAMWISE VORTEX: FLOW STRUCTURE AND SURFACE PRESSURE LOADING (S. Wolfe, J.-C. Lin and D. Rockwell, 1995, Journal of Fluids and Structures, Vol. 9, pp. 359-537)

This investigation addresses the impingement of a streamwise vortex on a thin plate. Breakdown of the incident vortex, which in this case occurs well upstream of the leading-edge, generates vortical structures that are distorted at the leading-edge

(Figure 4). The nature of this distortion is represented by instantaneous velocity and vorticity distributions over entire planes adjacent to the plate. The instantaneous distributions of vorticity show well-defined, large-scale concentrations along the boundary of the breakdown region, nominally located along the locus of maximum averaged vorticity (Figure 5). Correspondingly, the amplitudes of the surface pressure spectra at the leading-edge of the plate are largest when the location of maximum vorticity is aligned with the edge. The dominant frequency of the surface pressure on the plate is, however, insensitive to offset of the vortex axis relative to the leading-edge of the plate. On the other hand, global fluctuations of the entire region of vortex breakdown are sensitive to the offset of the incident vortex.

The major findings are described in further detail in the following:

(1) Pressure fluctuations at the leading-edge exhibit a sharply-defined peak, irrespective of the offset of the axis of the incident vortex, up to offsets of about one-half diameter of the vortex. These fluctuations are due to concentrations of negative and positive azimuthal vorticity. Although they exhibit irregularities in form and spatial position, these concentrations show a clearly-detectable wavelength (spacing) between them.

(2) The predominant frequency of the surface pressure is remarkably insensitive to offset of the vortex axis relative to the leading-edge of the plate. This observation should allow simplification of scaling criteria for predominant buffeting frequencies.

(3) The maximum amplitude of the pressure fluctuation at the leading-edge occurs when the locus of maximum (averaged) azimuthal vorticity within the region of vortex breakdown impinges upon the pressure tap at the leading-edge. In contrast, when the center of the vortex impinges on the leading-edge of the plate, the fluctuation levels are relatively low; correspondingly, the central region of the vortex breakdown region is essentially devoid of averaged vorticity. This observation suggests that deflection of the vortex by the order of only one-half its characteristic diameter, via control techniques, can substantially reduce the level of pressure fluctuations along the leading-edge.

(4) For a certain range of offset of the axis of the incident vortex relative to the leading-edge of the plate, large amplitude, low frequency, global oscillations of the entire region of vortex breakdown occur; during such oscillations, there are substantial streamwise excursions of the onset of vortex breakdown.

3.3 *BUFFETING OF FIN: DISTORTION OF INCIDENT VORTEX (S. Canbazoglu, J.-C. Lin, S. Wolfe and D. Rockwell, 1995, AIAA Journal, Vol. 33, No. 11, November, pp. 2144-2150)*

The encounter of a broken-down vortex with the swept leading-edge of a fin (Figure 6) is investigated in a water channel using high-image-density particle image velocimetry, which leads to instantaneous fields of velocity and vorticity. The vortex-fin interaction (Figure 7) generates a layer of time-averaged vorticity extending along the entire leading-edge from the root to the tip of the fin. This averaged vorticity is actually

due to a succession of instantaneous states of highly concentrated vorticity along the edge of the post-breakdown region of the vortex. Above the surface of the fin, however, the averaged vorticity has a relatively low level; the corresponding instantaneous vorticity concentrations have alternating sign and are not repetitive in space or time. Nevertheless, two-dimensional correlations of instantaneous vorticity exhibit well-defined peaks corresponding to an identifiable wavelength between the vorticity concentrations. Spectra of surface pressure at crucial locations on the fin are related to these features of the instantaneous and averaged flow structure.

More specifically, the central findings in this investigation are:

(1) The instantaneous structure of the broken-down vortex upstream of the leading-edge of the fin exhibits the classical staggered pattern of alternating positive and negative concentrations of vorticity. Along the leading-edge of the fin, however, including the edge of the tip, negative concentrations of vorticity dominate; they are due to a separated mixing-layer flow along the edge of the fin.

(2) Averaging of these instantaneous vorticity concentrations shows that a time-averaged, negative vorticity layer exists along the leading-edge and tip of the fin.

(3) Over the surface of the fin, the levels of fluctuating vorticity are significantly lower than those on the edge, at least in the region close to the fin surface. Correspondingly, averaged levels of vorticity are insignificant relative to those along the edge.

(4) Levels of fluctuating vorticity, obtained from a large number of instantaneous images, show regions of low and high levels of $\tilde{\omega}_{rms}$ vorticity that are in good agreement with regions of low and high rms surface pressure.

(5) Spectra of surface pressure fluctuations show peak values that, again, are well correlated with regions of high fluctuating vorticity. Although the frequency at which this peak occurs is unaltered in the leading-edge and tip region, there is substantial broadening and distortion of the energy content of the fluctuations in the central region of the fin. In this region, the instantaneous vorticity contours show both positive and negative contributions, appearing randomly from one instantaneous image to the next, and having substantially lower levels than those negative contours along the edge of the fin.

3.4 BUFFETING OF A FIN: STREAMWISE EVOLUTION OF FLOW STRUCTURE
(S. Canbazoglu, J.-C. Lin, S. Wolfe, and D. Rockwell, 1996, AIAA Journal of Aircraft (in press))

The encounter of a broken-down vortex with a fin (Figure 8) is characterized using high-image-density particle image velocimetry, which provides instantaneous and averaged representations of the distorted flow structure (Figure 9). Averaged patterns of sectional streamlines and streamwise vorticity show well-defined, large-scale vortical motions having vorticity of the same orientation as, and counter to, the incident vortex.

The counter-vortex, generated at the inclined leading-edge of the fin, exhibits substantial values of vorticity and circulation. Corresponding instantaneous images show pronounced concentrations of streamwise vorticity, which can have peak vorticity levels and values of circulation that exceed the averaged values by factors of three to five. The location and form of these vorticity concentrations vary randomly with time.

The primary findings are:

(1) In the leading-region of the fin, a counter-vortex, having a sense opposite to that of the incident vortex, is formed on the outboard side of the fin. Further downstream, at locations corresponding to the mid- and trailing-regions along the fin, this counter-vortex becomes less coherent and loses its identifiable structure.

(2) On the far outboard side of the fin, the averaged vorticity takes the form of a relatively thin shear layer, which feeds into a large-scale, broadly distributed vortex on the inboard side. This basic pattern persists all the way to the trailing-end of the fin, where only the averaged inboard vortex is identifiable.

(3) All of the foregoing features of the averaged vortices are actually made up of an array of highly concentrated positive and negative vorticity, whose form and spatial location change substantially from one instant to the next. The maximum vorticity levels of these concentrations are typically a factor of three to five higher than those of corresponding regions of averaged vorticity.

(4) Evaluation of distributions of root-mean-square fluctuating vorticity over the entire crossflow plane shows that the highest levels typically occur near the tip of the mid-region of the fin.

3.5 BUFFETING OF FINS: AN ASSESSMENT OF SURFACE PRESSURE LOADING (S. Wolfe, S. Canbazoglu, J.-C. Lin and D. Rockwell), 1995, AIAA Journal, Vol. 33, No. 11, pp. 2232-2234)

Consideration of a number of wind- and water-tunnel tests of buffeting of fins/tails, which focused on characterization of the time-averaged spectra of surface pressure fluctuations, shows that simple scaling criteria based on global features of the vortex breakdown provide a basis for scaling the predominant, dimensionless frequency of the buffeting phenomenon. These considerations reinforce the validity of low-speed experiments on buffeting phenomena occurring at relatively high speeds.

3.6 INTERACTIONS OF A VORTEX WITH AN OSCILLATING LEADING-EDGE (R. W. Jefferies and D. Rockwell, 1996, AIAA Journal, submitted for publication)

This investigation addresses the detailed structure of the interaction of an incident vortex with a leading-edge that is sinusoidally oscillating at the frequency of the incident vortex street. The instantaneous streamline patterns and vorticity distributions allow characterizations of the mechanisms of interaction, as a function of timing, or phase shift, of the incident vortex relative to the motion of the edge. Use of the high image-density technique of particle image velocimetry provides highly resolved representations of the

6

streamline topology in the vicinity of the leading-edge. The major findings in this investigation are that a proper phase shift between the incident vortex and the motion of the tip of the edge can yield a drastic decrease in the circulation of the secondary vortex formation from the tip of the edge. On the other hand, this phase shift technique also allows substantial enhancement of the secondary vortex formed from the tip of the edge. These results provide a basis for possible active control of vortex-leading-edge interactions.

3.7 *CINEMATOGRAPHIC SYSTEM FOR HIGH-IMAGE-DENSITY PARTICLE IMAGE VELOCIMETRY (J.-C. Lin and D. Rockwell, 1994, Experiments in Fluids, Vol. 17, pp. 110-114)*

A cinematographic system, which integrates the concepts of high-image-density PIV, laser scanning, and framing photography, allows temporal resolution of the order of one percent of the time scale of the largest vortical structures in the turbulent wake from a cylinder at a Reynolds number of 10,000. With this resolution in time, it is possible to track, in a continuous fashion, the patterns of streamwise vorticty in the near-wake. This system has general application to a wide variety of unsteady flows.

4. PERSONNEL SUPPORTED

Stephen Wolfe	M.Sc. Degree (1994)
Alejandro Mayori	M. Sc. Degree (1993)
Suat Canbazoglu	Visiting Scientist (funded almost entirely by Turkish government)
Jung-Cheng Lin	Research Associate

5. PUBLICATIONS

Canbazoglu, S., Lin, J.-C. Wolfe, S. and Rockwell, D. 1995 "Buffeting of Fin: Distortion of Incident Vortex", *AIAA Journal*, Vol. 33, No. 11, pp. 2144-2150.

Canbazoglu, S., Lin, J.-C., Wolfe, S. and Rockwell, D. 1995 "Buffeting of a Fin: Streamwise Evolution of Flow Structure", *AIAA Journal of Aircraft* (in press).

Jefferies, R. W. And Rockwell, D. 1996 "Interactions of a Vortex with an Oscillating Leading-Edge", *AIAA Journal* (submitted for publication).

Mayori, A. and Rockwell, D. 1994 "Interaction of a Streamwise Vortex with a Thin Plate: A Source of Turbulent Buffeting", *AIAA Journal*, Vol. 32, No. 10, pp. 2022-2029.

Wolfe, S., Canbazoglu, S., Lin, J.-C. and Rockwell, D. 1995 "Buffeting of Fins: An Assessment of Surface Pressure Loading", *AIAA Journal*, Vol. 33, No. 11, pp. 2232-2234).

Wolfe, S., Lin, J.-C. and Rockwell, D. 1995 "Buffeting of the Leading-Edge of a Flat Plate due to a Streamwise Vortex: Flow Structure and Surface Pressure Loading", *Journal of Fluids and Structures*, Vol. 9, pp. 359-370.
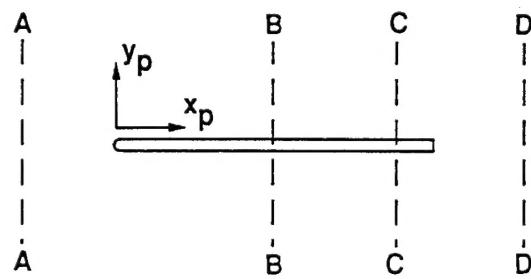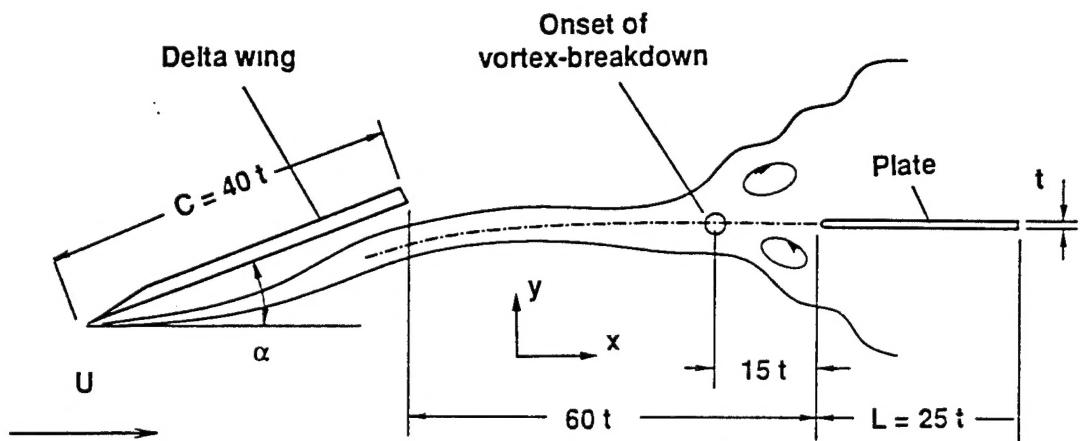
**Figure 1**: Schematic of experimental arrangement.

Onset of
vortex-breakdown

U

Vortex trajectory
above plate

Plate

Chaotic Flow

Onset of
vortex-breakdown

Vortex trajectory
below plate

Initial region
of vortex
splitting

Region of split
vortex development:
movement away from
plate surface and
plane of symmetry

Free interaction
region of split vortices
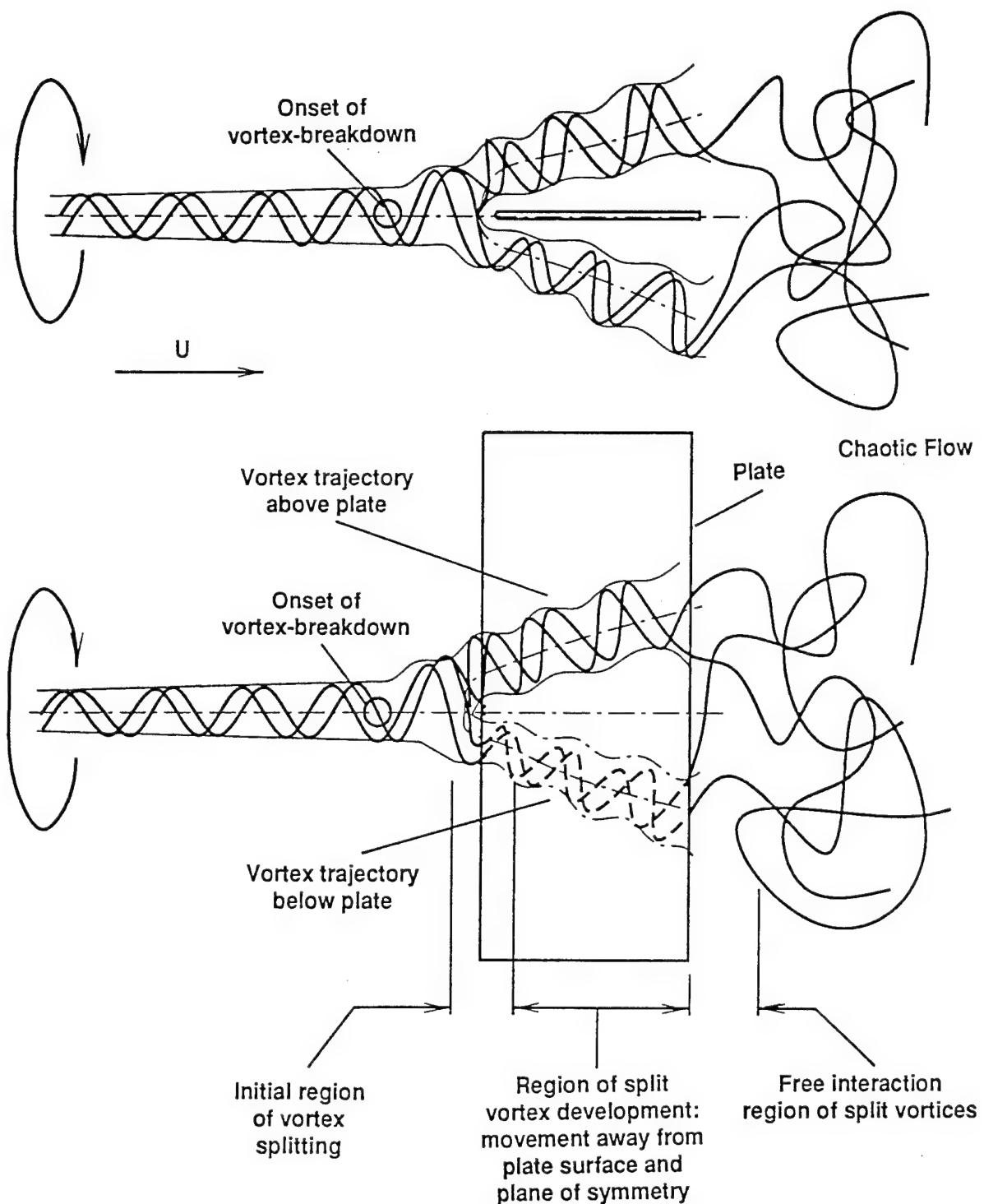
Figure 2: Overview of principal features of vortex breakdown-plate interaction.
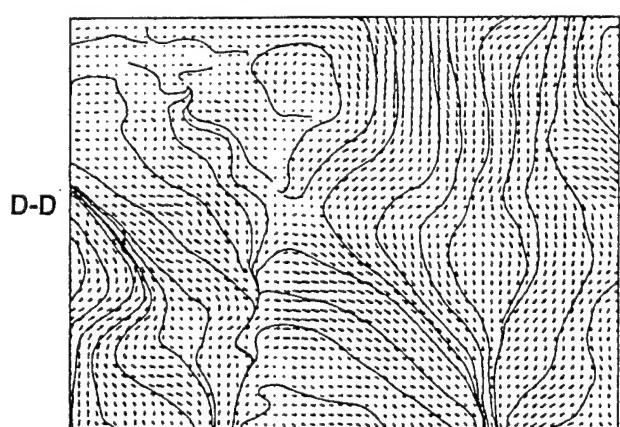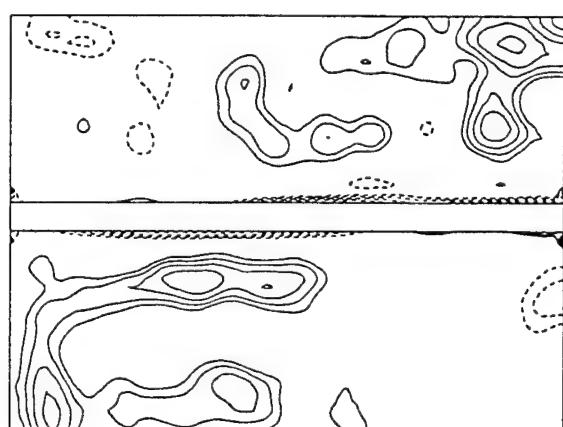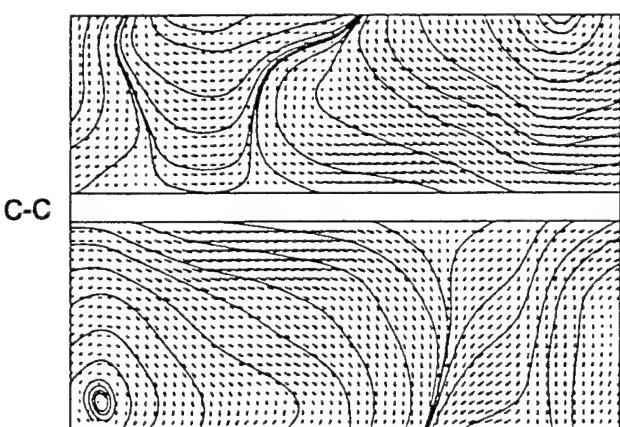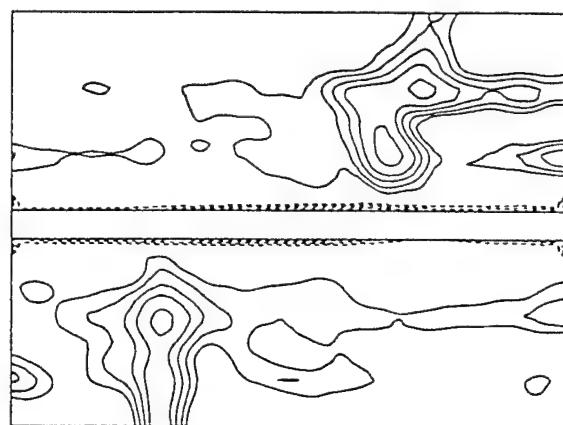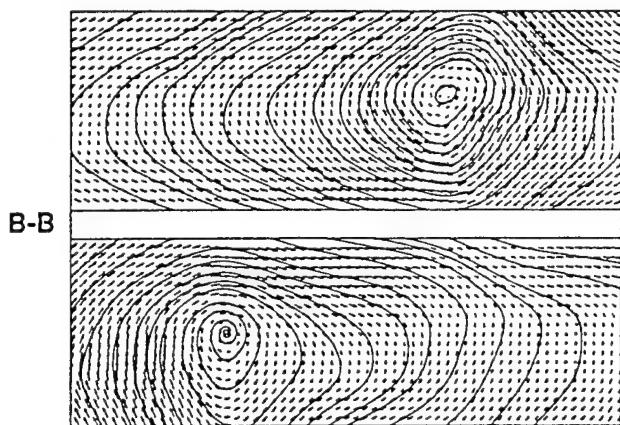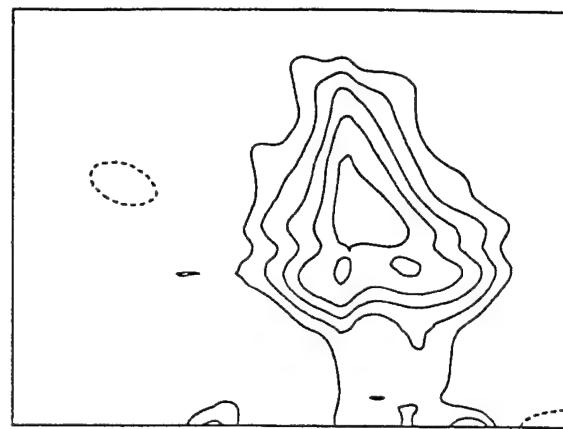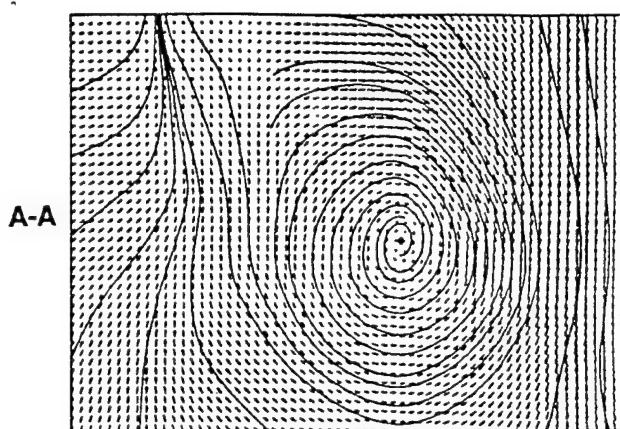
Figure 3: Time-averaged images of streamlines and contours of constant vorticity ω_x in various crossflow planes: A-A (upstream of leading-edge of plate); B-B at midchord of plate; C-C (at trailing-edge of plate); and D-D (downstream of plate). Positive and negative ω_x represented by solid and dashed lines respectively.
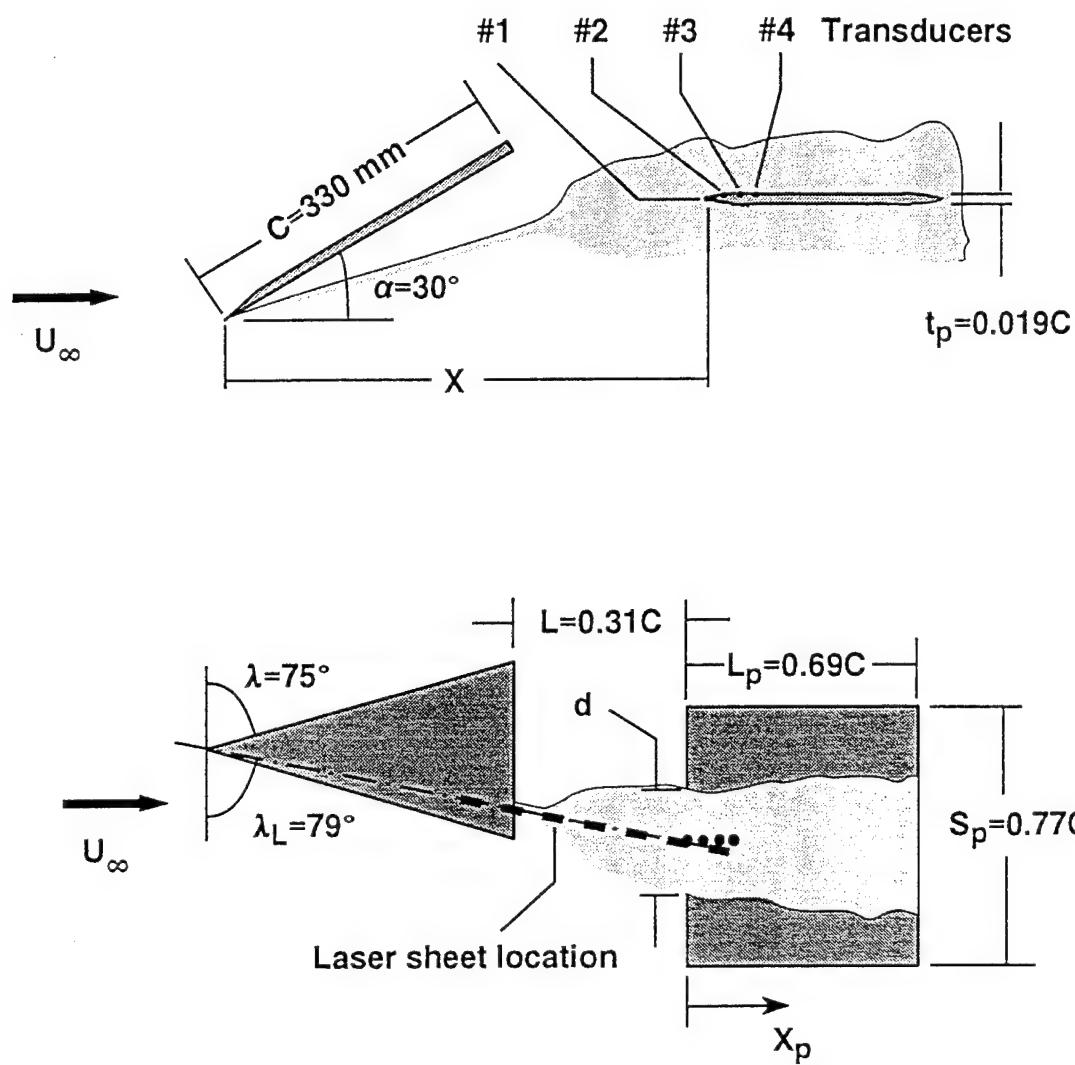
Figure 4: Overview of experimental arrangement.
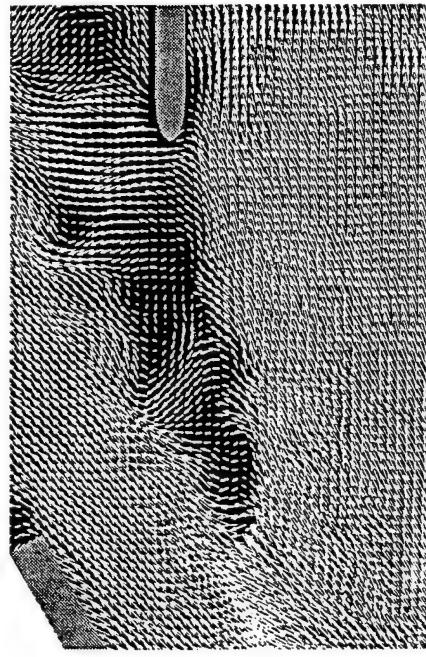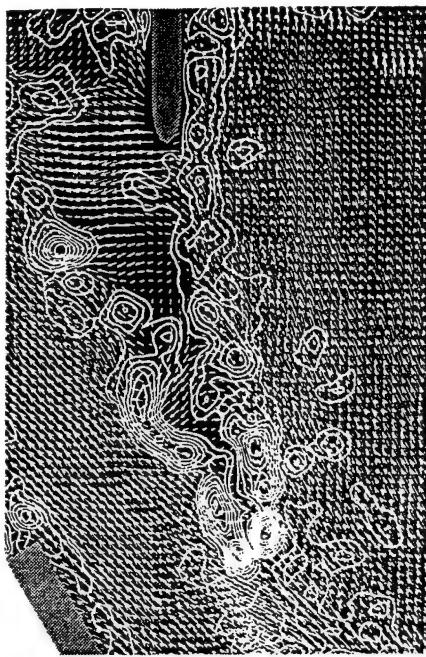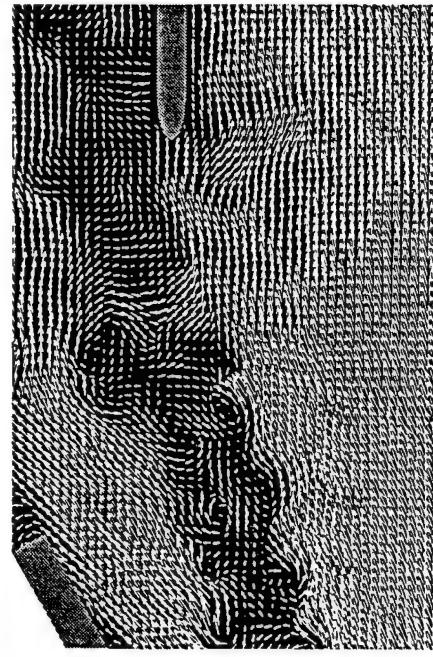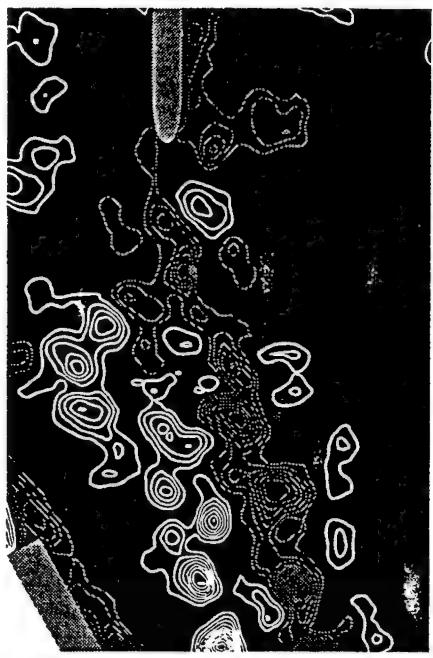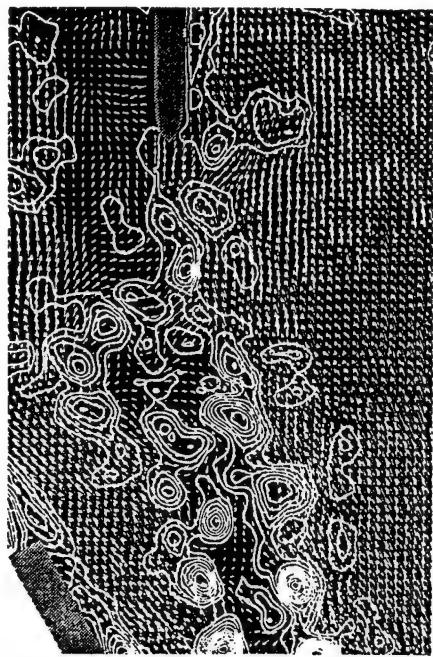
Figure 5: Instantaneous images of velocity vectors (left column), contours of constant vorticity ω_z (middle column), and velocity vectors on contours of constant vorticity (right column) for cross-stream distances $\eta/d = 0.26$ at two instants of time. Minimum vorticity $\omega_{min} = 5$ s^{-1} and incremental vorticity $\Delta\omega = 5$ s^{-1}.

Instant #1

Instant #2

330 mm

75°

11°

Δ

Laser sheet

Field of View

97 mm

76 mm

C_F=105 mm

(a)

α=25°

#5

#4

#1

#2,3

1.09C_F

0.98C_F

0.70C_F

0.62C_F

Struts

70°

57.5°

45°

C_F

(b)
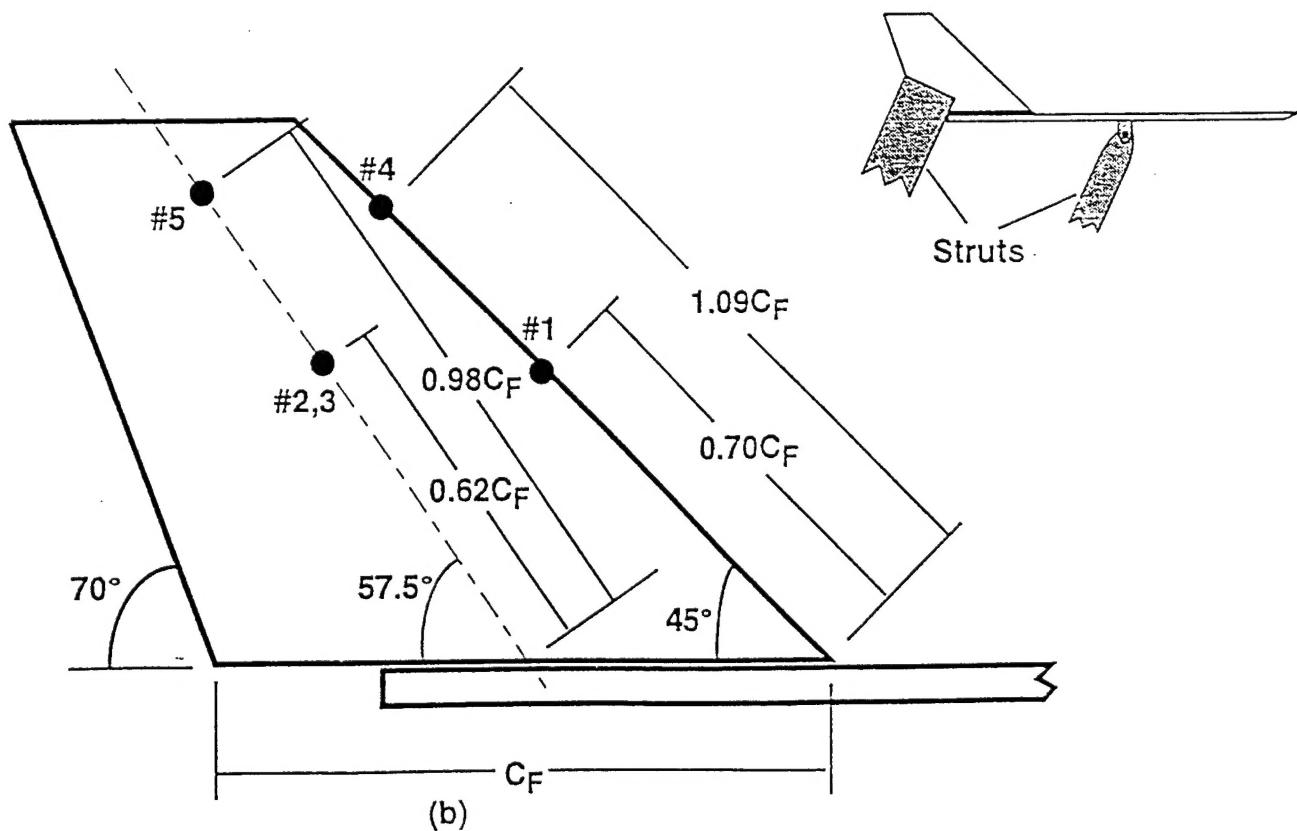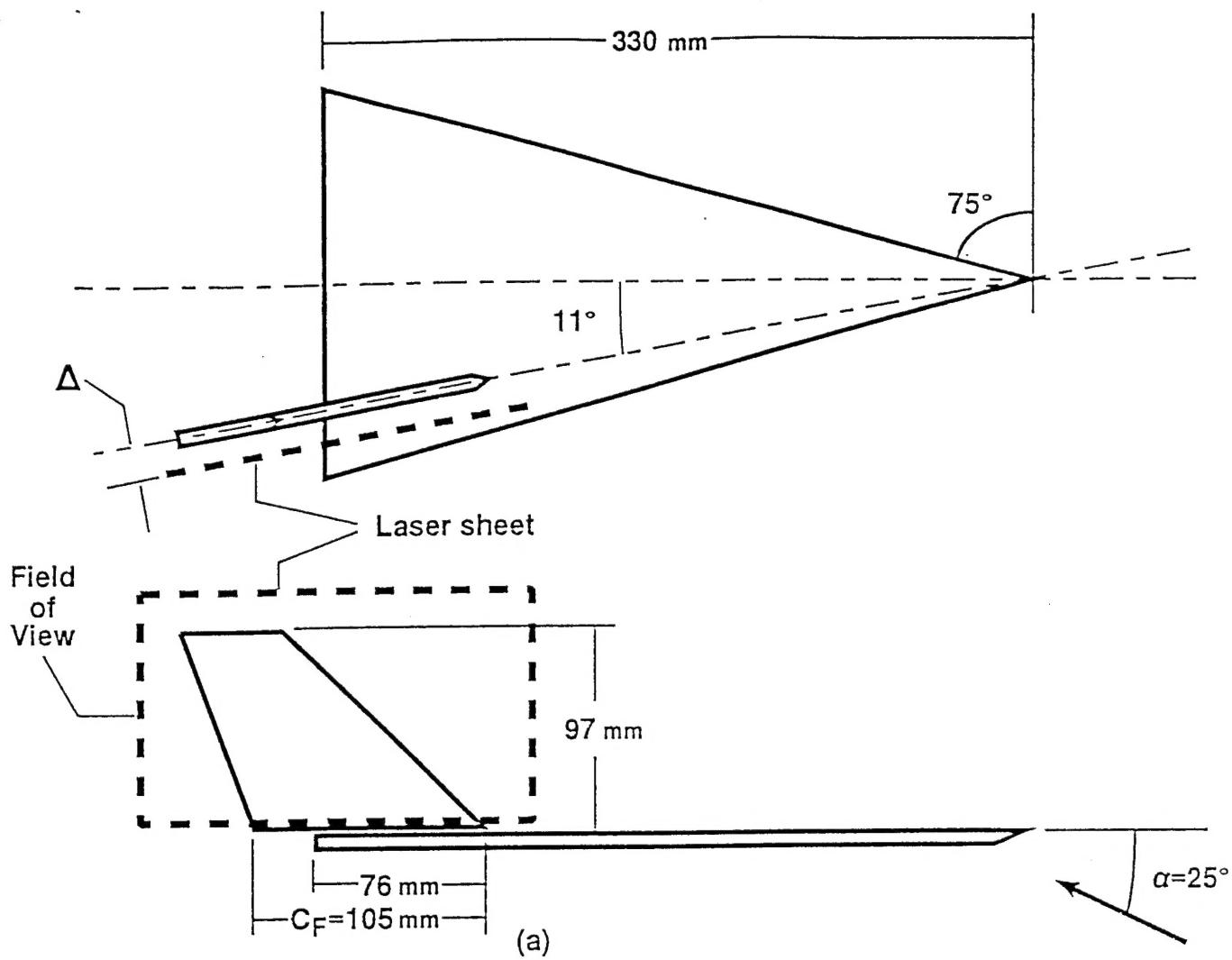
Figure 6: Overview of delta wing-fin system.

$\Delta^* = 0$ $\Delta^* = 0.06$
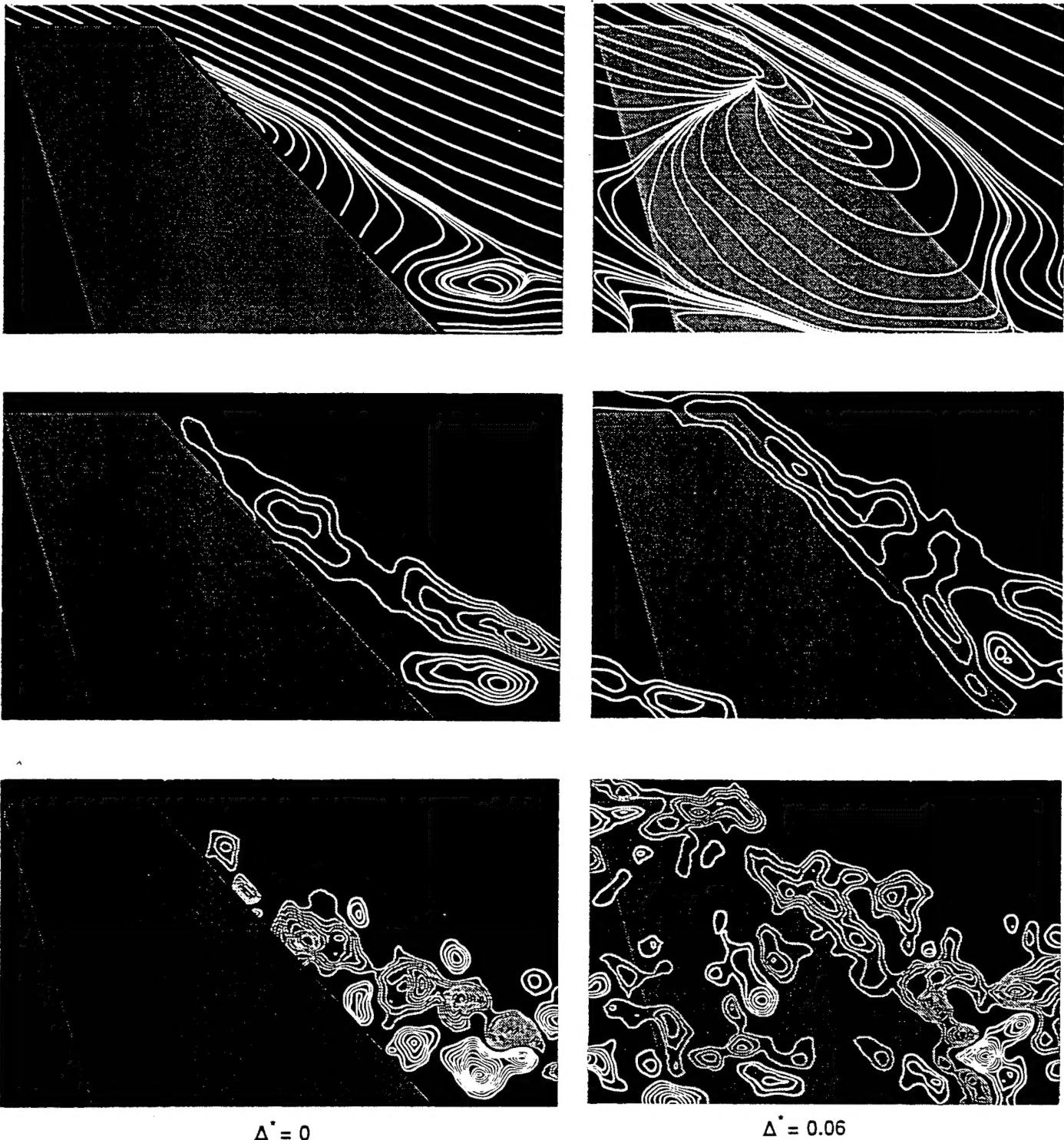
Figure 7: Averaged streamline patterns (top row), contours of constant vorticity (middle row), and instantaneous vorticity contours (bottom row) as a function of dimensionless distance Δ^* from surface of fin. For averaged and instantaneous vorticity contours, minimum and incremental levels of vorticity are ± 5 1/s and 3 1 /s respectively.
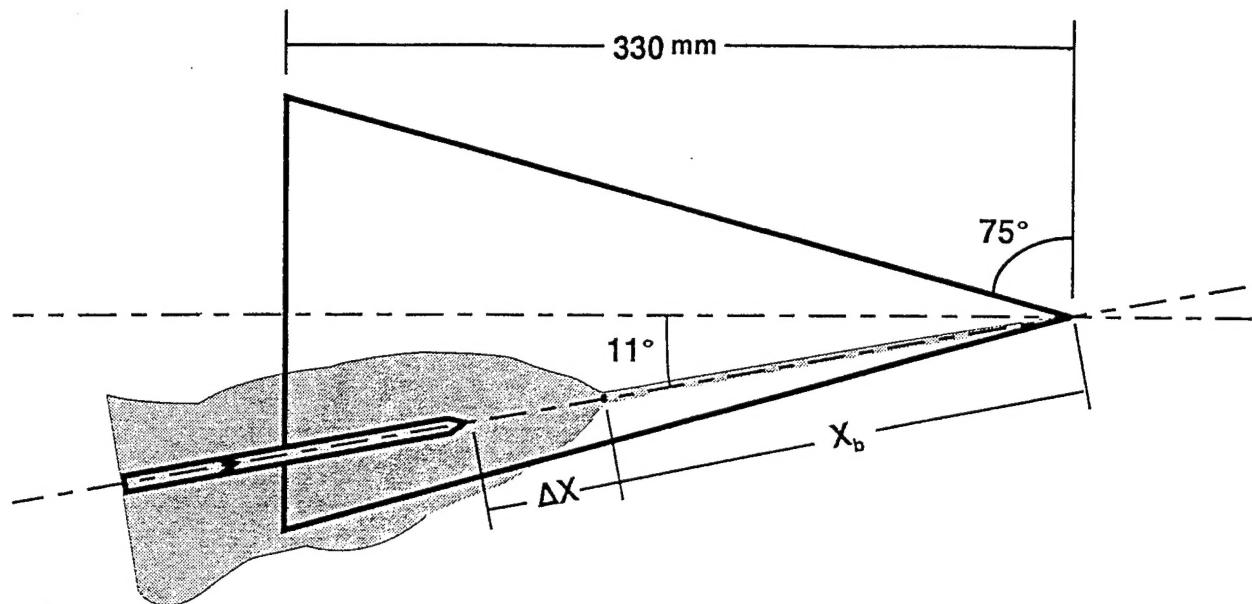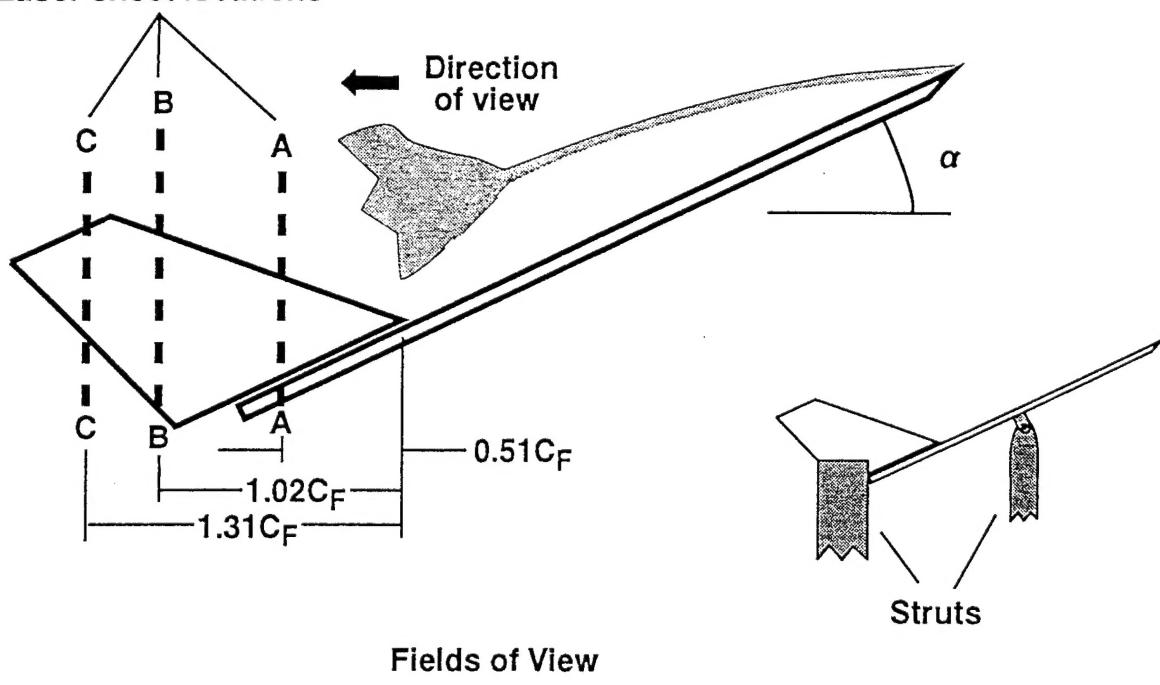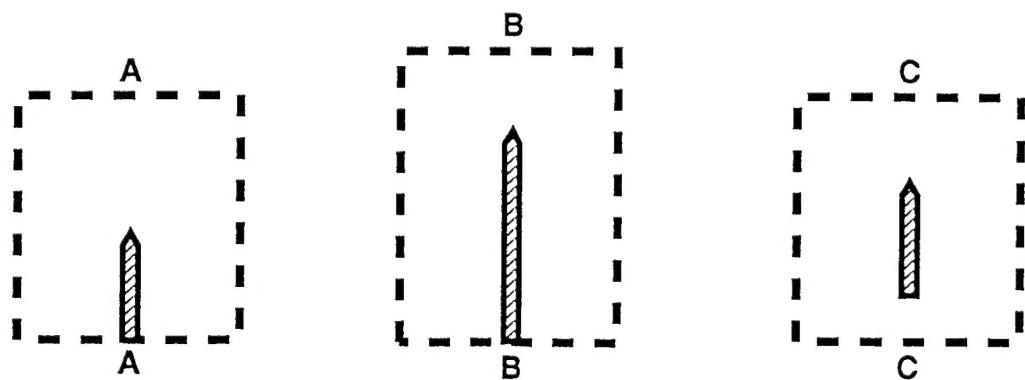
Figure 8: Overview of delta wing-fin system.
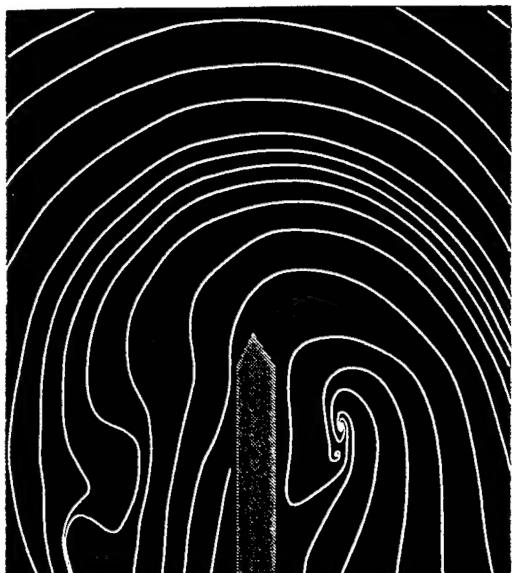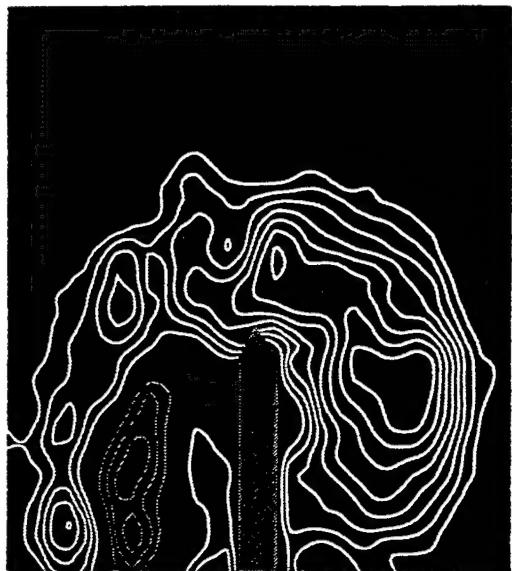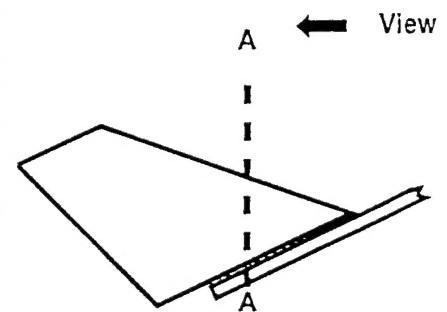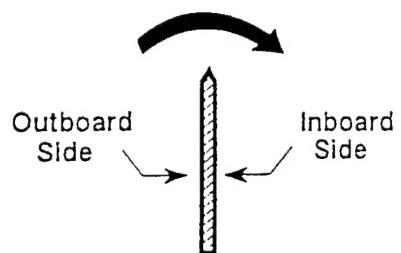
Figure 9: Cross-section of vortex-fin interaction in leading-region of fin showing (a) averaged streamlines; (b) averaged vorticity contours; and (c,d) instantaneous vorticity contours. For averaged vorticty contours, minimum and incremental levels of vorticity are ±5 1/s and 1 1/s respectively; for instantaneous contours, ±2.5 1/s and 2.5 1/s.